Polyhedron 153 (2018) 234–239

Contents lists available at ScienceDirect

Polyhedron

journal homepage: www.elsevier.com/locate/poly

Loading and release of the complex [Pt(DTBTA)(DMSO)Cl]Cl·$CHCl_3$ with the 2,2′-dithiobis(benzothiazole) ligand into mesoporous silica and studies of antiproliferative activity on MCF-7 cells

Simona Rubino [a,*], Maria Luisa Saladino [a,b,*], Rosalia Busà [a], Delia Francesca Chillura Martino [a,b], Maria Assunta Girasolo [a], Eugenio Caponetti [a,b], Luisa Tesoriere [a], Alessandro Attanzio [a]

[a] Dipartimento di Scienze e Tecnologie Biologiche, Chimiche e Farmaceutiche (STEBICEF) and INSTM UdR – Palermo, Università di Palermo, Viale delle Scienze Ed. 17, Parco d'Orleans II, 90128 Palermo, Italy
[b] Polo Centro Grandi Apparecchiature-ATeN Center, Università di Palermo, Via F. Marini 14, Palermo I-90128, Italy

ARTICLE INFO

Article history:
Received 24 April 2018
Accepted 6 July 2018

Keywords:
Loading
Controlled release
MCM41
Platinum(II) complex
Antiproliferative activity

ABSTRACT

Synthetic delivery systems have great potential for overcoming problems associated with systemic toxicity that accompanies chemotherapy with the use of cisplatin and family of platinum anticancer drugs. Mesoporous silicates have been studied in context of drug delivery and drug targeting. In this paper we report the studies of loading and release of a platinum complex, [Pt(DTBTA)(DMSO)Cl]Cl·$CHCl_3$ (1) where DTBTA = 2,2′-dithiobis(benzothiazole), that was recently synthesized and structurally characterized. Evaluation *in vitro* of antitumor activity against a human breast cancer cell line (MCF-7) showed a very potent activity of complex(**1**). Therefore, we thought to incorporate this compound into MCM41 mesoporous silica and into analogous support functionalized with amino groups (MCM41-NH_2). The complex(**1**) encapsulation efficiency % (EE%) in MCM41 and in MCM41-NH_2, respectively, was evaluated by using UV–Vis spectroscopy. The porosimetry and IR spectra confirmed that the drug was within the pores in MCM-41 and that the complex(**1**) binds MCM41-NH_2 with the aminopropyl functional groups of the mesoporous channels, respectively. The study of release was performed by using UV–Vis spectroscopy at 37 ± 1 °C in 0.1 M phosphate buffer solution (PBS) having pH 7.4 to simulate the physiological pH of blood. In order to investigate the efficacy of MCM-41/complex(**1**) and MCM41-NH_2/complex(**1**) conjugates, we have measured their ability to kill cancer cells of MCF-7 (human breast cancer). MTT test and cytofluorimetric assay of exposure of phosphatidylserine to the outer membrane were carried out to measure cytotoxicity and apoptosis induced by MCM41/complex(**1**) and MCM41-NH_2/complex(**1**). The investigated systems were very efficient for pharmaceutical controlled release and a promising agent for combination therapies.

1. Introduction

Cisplatin has been one of the most active antitumor agents in current clinical use, being curative in the treatment of ovarian, testicular, bladder, cervical, head, neck and non-small cell lung cancers. In past and recent years, an intensive research has led to the synthesis of thousands of new platinum compounds with the aim of overcoming cisplatin toxicity and resistance and improving its efficacy [1,2]. Cisplatin has a number of side effects, such as nephrotoxicity, nausea, vomiting, myelosuppression, ototoxicity, and neurotoxicity that can limit its use. Nephrotoxicity results from injury to renal tubular epithelial cells and can be manifested as either acute renal failure or a chronic syndrome characterized by

Abbreviations: TEOS, tetraethoxysilane; CTAB, cetyltrimetylammonium bromide; APTES, 3-aminopropyltriethoxysilane; BTA, benzothiazole; MTT, 3-(4,5-dimethyl-2-thiazolyl)bromide-2,5-diphenyl-2H-tetrazolium; DMSO, dimethylsulfoxide; PI, propidium iodide; FACS, fluorescence-activated cell sorting; FBS, fetal bovine serum; MTT, 3-(4,5-dimethyl-2-thiazolyl)bromide-2,5-diphenyl-2H-tetrazolium; PBS, phosphate buffer; PS, phosphatidylserine; RPMI, Roswell Park Memorial Institute.

* Corresponding authors at: Dipartimento di Scienze e Tecnologie Biologiche, Chimiche e Farmaceutiche (STEBICEF) and INSTM UdR – Palermo, Università di Palermo, Viale delle Scienze Ed. 17, Parco d'Orleans II, 90128 Palermo, Italy (M.L. Saladino). Fax: +39 091 6577270.

E-mail addresses: simona.rubino@unipa.it (S. Rubino), marialuisa.saladino@unipa.it (M.L. Saladino).

https://doi.org/10.1016/j.poly.2018.07.006
0277-5387/

renal electrolyte wasting [3]. These renal adverse effects are correlated to platinum binding and inactivation of thiol-containing enzymes [4]. Molecules containing sulphur are currently under study as chemo protectants in platinum-based drugs chemotherapy [5]. Among pharmacologically important heterocyclic compounds, Benzothiazole (BTA) and its derivatives are the most important heterocyclic compounds, which are common and integral feature of natural products and pharmaceutical agents and show a variety of pharmacological properties [6–8]. We have recently synthesized and structurally characterized a platinum(II) complex(**1**), [Pt(DTBTA)(DMSO)Cl]Cl·$CHCl_3$, showing the evaluation of its very potent *in vitro* antitumor activity against a human breast cancer cell line (MCF-7) [9]. Complex(**1**) in fact was effective inducer of apoptotic death on MCF-7 cells and causes cell arrest at G0/G1 phase. To reduce and overcame the toxicity of cisplatin and its analogues, we have thought to study a selective delivery of Pt (II)-based antitumor drug complex(**1**) obtained by loading it onto inorganic matrices. A wide variety of nanostructured and microstructured materials for biological and medical applications have been widely studied for delivery of small molecules and cisplatin was one of these small and active molecules [10–14]. Drug delivery systems are able to improve the permeability retention effect, safety, pharmacokinetics properties and bioavailability of the therapeutic substances in treatment of tumour [15]. MCM41 mesoporous silica was first proposed as drug delivery device in 2000 [16,17]. This mesoporous has a high surface area and pore volume that allows it to host a large amount of a determined biologically active molecule, while its ordered pore network allows fine control of the molecule load and release kinetics [18,19]. In this work we studied loading and release of Pt(II) complex(**1**) [Pt (DTBTA)(DMSO)Cl]Cl·$CHCl_3$ [9], on mesoporous silica MCM41 and mesoporous silica functionalized with amino groups (MCM41-NH_2). The mechanism of anchoring of complex(**1**) onto the silica support materials was reported. Then the *in vitro* cytotoxicity and pro-apoptotic efficacy of complex(**1**) loaded on MCM41 [MCM41/complex(**1**)] or MCM41-NH_2 [MCM41-NH_2/complex(**1**)], was studied on MCF7 cell line.

2. Experimental

2.1. Materials and general experimental conditions

Tetraethoxysilane (TEOS, 99%, Fluka), cetyltrimetylammonium bromide (CTAB, 98%, Aldrich), ammonia solution (28%, Aldrich), ethanol (99.8%, Fluka), 3-aminopropyltriethoxysilane (APTES 98%, Aldrich), anhydrous toluene (99.8%, Aldrich), diethyl ether (99.9%, Aldrich), dichloromethane (99.5%, Aldrich), chloroform (99.5%, Aldrich), DMSO (99.7%, Aldrich) were used as received. The phosphate buffer solution (PBS, 0.1 mol/L^{-1}, pH 7.4) were prepared mixing 8.0 g of NaCl, 2.38 g of Na_2HPO_4 and 0.19 g of KH_2PO_4 in 1 L of deionised water. Solutions were prepared by weight adding conductivity grade water.

Recently, the synthesis of complex(**1**) from cis-[$PtCl_2(DMSO)_2$] in chloroform solution and its full characterization was reported [9]. The syntheses of the MCM41 and MCM41-NH_2 mesoporous silica were also reported [20–22]. The used MCM-41 has a highly-ordered hexagonal structures with toroidal particles of a few microns in size. The structure of the amino functionalized MCM41 with functionalization degree of 63% is analogues to the ones of MCM41.

2.2. Characterization

UV–Vis absorption spectra of solutions of complex(**1**) were recorded in the range 200–600 nm using a double beam Beckman DU-800 spectrophotometer with a resolution of 1.0 nm. In order to eliminate the effect of particle diffusion, the value of absorbance at 600 nm was subtracted to each spectrum. For calibration purposes, six solutions of complex(**1**) were prepared in chloroform in the range of 0.004–0.03 mg/mL. The UV–Vis spectra of the standard solutions were reported in Fig. SI1 of the Support Information (S. I.). The calibration curve, obtained by plotting the absorbance values of the band maximum (λ_{max} = 310 nm) versus the solution concentrations, was reported in Fig. SI2 of the S.I.

N_2 absorption–desorption isotherms were registered at 77 K using a Quantachrome Nova 2200 Multi-Station High Speed Gas Sorption Analyser. Samples were out gassed for 12 h at room temperature in the degas station. Adsorbed nitrogen volumes were normalized to the standard temperature and pressure. The S_{BET} was calculated by using the BET method [23] in the relative adsorption pressure (P/P_0) range from 0.045 to 0.250. The V_t was obtained from the nitrogen amount adsorbed in correspondence of P/P_0 equal to 0.99.

The ATR spectra were recorded in the 40–4000 cm^{-1} range, with a step of 2 cm^{-1}, by using a FT-IR Bruker Vertex 70 Advanced Research Fourier Transform Infrared Spectrometer equipped with Platinum ATR.

2.3. Loading of complex(*1*) on MCM41 and MCM41-NH_2

The complex(**1**) loading was performed by following the experimental procedure reported by us [24], the mesoporous silica powders were soaked, under continuous magnetic stirring for 24 h at room temperature, into a chloroform solution of complex(**1**) (0.06 mg/mL). The mesoporous quantity was 83.3 mg for gram of complex(**1**). The loaded samples were recovered by vacuum filtration, washed with chloroform and dried under vacuum overnight. The supernatant was collected and analysed by using UV–Vis spectroscopy to determine the unloaded amount of complex(**1**) and by difference, the loaded quantity on the mesoporous. The drug encapsulation efficiency % (EE%) of mesoporous samples was evaluated as 100 * (total drug added − free non-entrapped drug)/(total drug added).

2.4. Cell lines

Cell lines of MCF-7 (human breast cancer) were purchased from American Type Culture Collection, Rockville, MD, USA. Cells were grown in RPMI medium supplemented with L-glutamine (2 mM), 10% fetal bovine serum (FBS), penicillin (100 U/mL), streptomycin (100 μg/mL) and gentamicin (5 μg/mL) and maintained in log phase by seeding twice a week at a density of 3×10^8 cells/L in humidified 5% CO_2 atmosphere, at 37 °C.

2.5. In vitro cytotoxicity assays of MCM41/complex(*1*) and MCM41-NH_2/complex(*1*)

MCM41/complex(**1**), MCM41-NH_2/complex(**1**) or complex(**1**) were dissolved in DMSO and then diluted in RPMI so that the effective DMSO and drug concentrations were 0.1% and 1 μM, respectively. Comparable solutions of unloaded MCM41 and MCM41-NH_2 were also prepared. Cytotoxicity of MCM41/complex(**1**) and MCM41-NH_2/complex(**1**) was tested in MCF-7 cells using the MTT colorimetric assay based on the reduction of 3-(4,5-dimethyl-2-thiazolyl)bromide-2,5-diphenyl-2H-tetrazolium (MTT) to purple formazan by mitochondrial dehydrogenases of living cells. This method is commonly used to illustrate inhibition of cellular proliferation. Briefly, cells were seeded in a 96-well plate at a density of 5000 cells/well containing 200 μL RPMI and allowed to adhere for 24 h. Then cells were washed with fresh medium and incubated with the mesoporous loaded or

unloaded samples, complex(**1**) or vehicle alone (control cells) in RPMI. After a 48 or 72 h incubation, cells were washed, and 50 μL FBS-free medium containing 5 mg/mL MTT were added. The medium was discarded after 2 h incubation at 37 °C by centrifugation, and formazan blue formed in the cells was dissolved in DMSO. The absorbance, measured at 570 nm in a microplate reader (Bio-RAD, Hercules, CA), of MTT formazan of control cells was taken as 100% of viability. Each experiment was repeated at least three times in triplicate to obtain the mean values. No differences were found between cells treated with DMSO 0.1% and untreated cells in terms of cell number and viability.

2.6. Measurement of phosphatidylserine exposure

The externalization of phosphatidylserine (PS) to the cell surface was detected by flow cytometry by double staining with Annexin V-Fluorescein isothiocyanate (Annexin V-FITC)/propidium iodide (PI). Phosphatidylserine, which was normally located on the cytoplasmic surface of cell membranes, was exposed on the cell surface upon induction of apoptosis. Annexin V binds to phosphatidylserine and was used to identify the earliest stage of apoptosis. PI, which does not enter cells with intact membranes, was used to distinguish between early apoptotic cells (Annexin V-FITC positive and PI negative) and late apoptotic cells (Annexin V-FITC/PI-double positive). MCF-7 tumor cells were seeded in triplicate in 24-wells culture plates at a density of 2.0×10^4 cells/cm^2. After an overnight incubation, the cells were washed with fresh medium and incubated with MCM41/complex(**1**), MCM41-NH_2/complex (**1**) and complex(**1**) in RPMI. After 48 h, cells were harvested by trypsinization and adjusted at 1.0×10^6 cells/mL with combining buffer according to the manufacturer' instructions (eBioscience, San Diego, CA). One hundred μL of cell suspended solution was added to a new tube, and incubated with Annexin V-FITC and PI solution at room temperature in the dark for 15 min. Then samples of at least 1.0×10^4 cells were subjected to fluorescence-activated cell sorting (FACS) analysis by Epics XL™ flow cytometer using Expo32 software (Beckman Coulter, Fullerton, CA), using appropriate 2-bidimensional gating method.

3. Results and discussion

3.1. Characterization of complex(*1*) incorporated into MCM41 and the MCM41-NH_2 mesoporous silica

The EE% was 63.3 w/w% and 94.4 w/w% for the MCM41 and the MCM41-NH_2 samples, respectively (all loading measurements were performed in triplicate). The Nitrogen adsorption–desorption isotherms were reported in Figs. SI3 and SI4 of the S.I. According to IUPAC [25] the characteristic type IV-isotherms and type I-isotherms were obtained for the MCM41 and MCM41-NH_2 loaded samples and were similar to the ones of the unloaded supports. Similar results have been obtained for other drug loaded on the same supports [17,21,22]. S_{BET} and V_t were reported in Table 1. The used MCM41 has surface area of 1276 m^2 g^{-1}, mean pore width of 3.5 nm, and pore volume of 0.71 cm^3 g^{-1}, while the MCM41-NH_2 mesoporous silica has surface area of 87 m^2 g^{-1}, mean pore width of 3.7 nm and pore volume of 0.07 cm^3 g^{-1}. As expected, after the loading, the surface area and the pore volume of MCM41 significantly decrease (the values are 39% and 24% lower than the respective unloaded), indicating the presence of the drug within the pores. After the loading procedures the molecules of drug remain trapped partially obstructing the mesochannels, analogously to what reported by Zeng at al [26]. On the contrary, different results are obtained for the MCM41-NH_2 where the surface area unvaried.

Table 1
S_{BET}, specific surface area and Vt, total pore volume values obtained from the Nitrogen adsorption–desorption isotherms data analysis.

Sample	S_{BET} (m^2 g^{-1})*	V_t (cc/g)
MCM41	1276	1.35
MCM41/complex(**1**)	494	0.32
MCM41-NH_2	87	0.07
MCM41-NH_2/complex(**1**)	90	0.21

* The uncertainty on the S_{BET} values is 5%.

The IR spectra (Fig. 1 A, B) of MCM41/complex(**1**) and MCM41 are superimposable as a consequence of the strong, typical stretching and bending bands of MCM41 that cover the signals of the complex(**1**). From the above result, no reliable conclusion about the interactions between the complex(**1**) and the mesoporous support can be drawn. The spectrum of MCM41-NH_2/complex(**1**) showed a characteristic broad band at 1541 cm^{-1} and two little

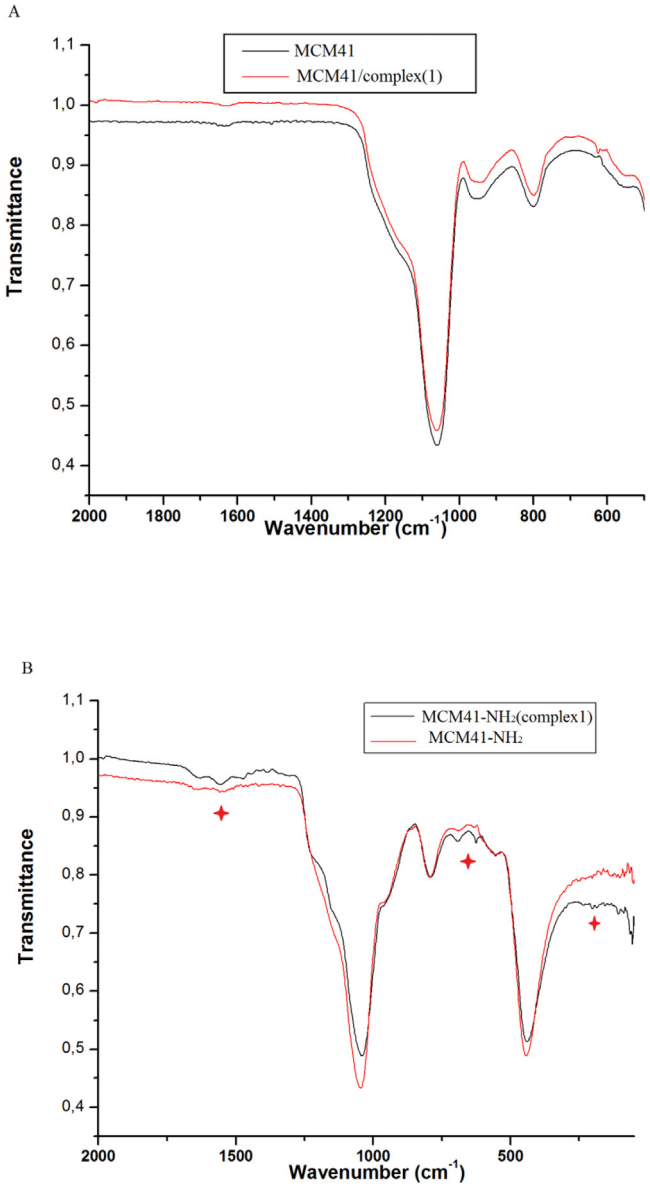

Fig. 1. FTIR spectra of (A) MCM41 and MCM41/complex(**1**), (B) MCM41-NH_2 and MCM41-NH_2/complex(**1**), ✦ major vibrational bands.

bands at 340 and 280 cm^{-1}. These bands were due to stretching vibration ν(C=N) of benzothiazole ring, ν(Pt–Cl) of Pt–Cl bond of the complex(**1**), ν(Pt–N) vibration of Pt-N bonds of the complex (**1**) and of the coordination bond between the lone pair of $-NH_2$ group and Pt(II) ion after dissociation of DMSO ligand [27].

The strongest absorption bands relative to the silica structure, appearing in the range between 1000 and 1300 cm^{-1}, were due to the bulk Si–O–Si groups asymmetric stretching vibration mode, whereas the peaks at 806 and 460 cm^{-1} were attributed to the Si–O–Si groups symmetric stretching and bending vibrations, respectively. The band at 966 cm^{-1} corresponded to the stretching vibration of Si–O–H surface groups. Finally, the band at 1652 cm^{-1} corresponded to ν(O–H) stretching vibration and δ(O–H) bending vibration of the O–H bond. Typical ν(C–H) stretching vibrations of the propyl chains at ca. 2900 cm^{-1} and δ(Si–CH_2) bending at 1385 cm^{-1}, together with $\delta(NH_2)$ bending band at ca.1570–1656 cm^{-1} for the MCM41-NH_2, confirmed the presence of alkyl chains and amino groups in the functionalized amino samples [28]. The stretching signals of the propyl groups and Si–O–Si groups, shifted toward higher wavenumbers, were considered an indication of the success of the functionalization. Furthermore, Si–C bonds stretching and bending signals at 2580 and 693 cm^{-1} confirmed the functionalization. In presence of the complex(**1**) these last vibrational modes were shifted to higher wavenumber indicating an interaction with the mesoporous. Looking for the surface area of the loaded sample, probably, MCM41 binds the complex(**1**) through host–guest supramolecular interaction with negligible effects on the IR vibrations, while the aminopropyl functional groups of the mesoporous channels of MCM41-NH_2 are able to bind the complex(**1**).

The mechanism of anchoring was proposed in Scheme 1.

3.2. Study of the release

The study of complex(**1**) release was performed at 37 ± 1 °C in 0.1 M phosphate buffer solution (PBS) having pH 7.4 to simulate the physiological pH of blood. 40 mg of the loaded samples were placed with 2 mL of PBS in a closed 3,5 kDa dialysis membrane tube (Spectra/Por 3 Dialysis membrane. 3,5 MWCO, 11,5 mm diameter), and then in a Nalgene-flask filled with PBS. The total amount of PBS was 20 mL. The flask was closed and kept under shaking (60 rpm) at 37 ± 1 °C. At scheduled time intervals, an aliquot of the solution was taken and the UV–Vis spectrum was recorded up to 120 h.

Six solutions of complex(**1**) in PBS were prepared, starting from a 1 mg/ml DMSO stock solution in the range of 0.005–0.05 mg/mL in order to obtain a calibration curve. The DMSO percentage of calibration and blank solutions was 3.0%. The UV–Vis spectra of the above solutions were reported in Fig. SI5 of the S.I. The calibration curve, obtained by plotting the absorbance values of the band maximum (λ_{max} = 308 nm) versus the solution concentrations, was reported in Fig. SI6 of the S.I.

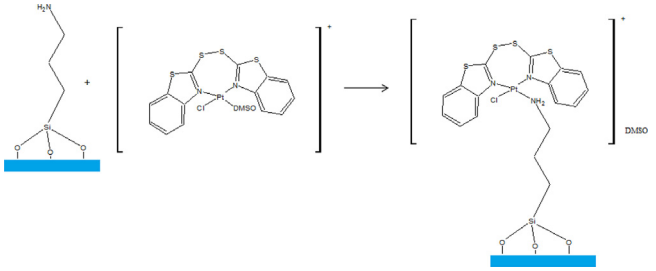

Scheme 1. Anchoring of [Pt(DTBTA)(DMSO)Cl]$^+$ onto the modified Silica surface.

The UV–Vis spectrum of each aliquot taken (in the range 0–120 h) by the PBS dispersion of MCM41-NH_2/complex(**1**) and the MCM41/complex(**1**) systems was reported in Figs. SI7 and SI8, respectively. The amount of released complex(**1**) was calculated by the maximum of the absorption band at 308 nm on the basis of the calibration curve. The release profile of complex(**1**) from both mesoporous was reported in Fig. 2.

The maximum released complex(**1**) ratio was 30.0% (2.3 mg for g of MCM41) at 24 h and 37.4% (4.2 mg for g of MCM41-NH_2) at 72 h. The released amount from the MCM41/complex(**1**) system reached the plateau concentration faster than MCM41-NH_2 system, according to the lower EE% and the IR spectra. In fact, even if the surface area decreasing confirms its presence in the mesoporous pores, the faster release could be considered an evidence of the absence of specific interactions between them, as suggested by the IR spectra. Probably, the main process involved in the loading and in the release is the diffusion toward the channels due to different affinity toward the two solvents. At the same time, the lower release proves the interaction between the amino groups of the mesoporous and the complex(**1**), which acts under its release in PBS. However, both systems are able to release the drug in an interval of time considered viable for a medical treatment [10]. This result is interesting even considering the opposite results obtained by loading a similar analogues of the cisplatin, the $[PtCl_2(DMSO)HL]\cdot 2DMSO$, where HL = 7-amino-2-(methylthio) [1,2,4]triazolo[1,5-a]pyrimidine-6-carboxylic acid, onto the same

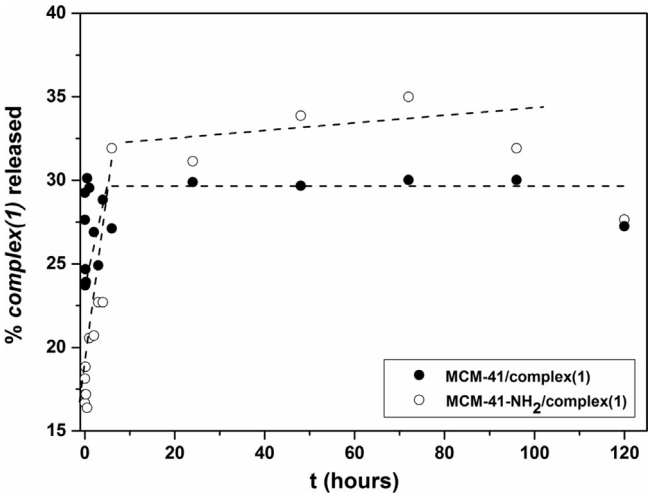

Fig. 2. Release profile of complex(**1**) in PBS solution from the MCM41/complex(**1**) and MCM41-NH_2/complex(**1**) samples.

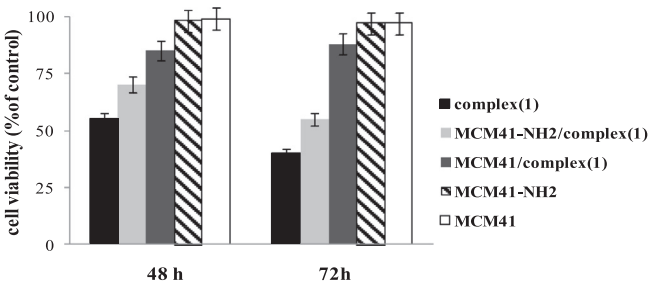

Fig. 3. *In vitro* cytotoxicity of MCM41-NH_2/complex(**1**) and MCM41/complex(**1**) on MCF-7 cells. Cells were treated with the loaded mesoporous silica or free complex (**1**) at 1 μM concentration. Cell treatment with solution of unloaded silica pounder was also carried out. Cell survival was measured after 48 or 72 h, by MTT assay in comparison to cells treated with vehicle alone (control), as reported in Section 2. Values are the mean ± standard deviation (SD) of three separate experiments carried out in triplicate.

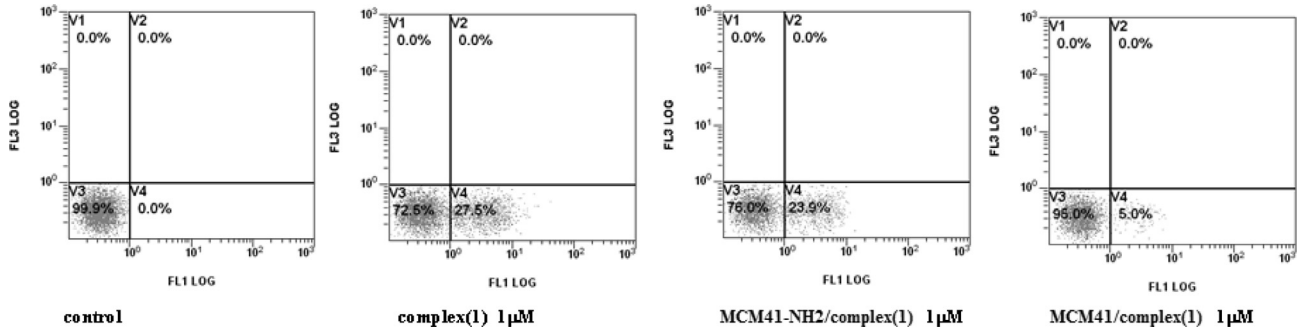

Fig. 4. Flow cytometric analysis for the quantification by AnnexinV/PI double staining of the MCM41-NH2/complex(**1**) and MCM41/complex(**1**) induced apoptosis in MCF-7 cells. Cell monolayers were incubated for 48 h in the absence (control) or in the presence of the loaded mesoporous silica or free complex(**1**) and submitted to double staining with Annexin V/PI as reported in Section 2. V3, viable cells (AnnexinV-/PI−); V4, cells in early apoptosis(AnnexinV+/PI−); V2, cells in tardive apoptosis (AnnexinV+/PI+); V1, necrotic cells (AnnexinV−/PI+). Representative images of three experiments with comparable results.

supports. In fact, the functionalized MCM41 showed slower drug release respect to the unfunctionalized material [23]. In that case, the different release kinetics has been explained by considering the formation of hydrogen bonds among the amino groups of functionalized silica and the carboxylic groups of the drug. These opposite results confirm the necessity to deepen the physical–chemical investigation of new analogues of the cisplatin drugs.

3.3. Cytotoxicity assay

MTT assay was used to investigate the *in vitro* cytotoxicity of MCM41/complex(**1**) and MCM41-NH_2/complex(**1**) on MCF-7 cells in comparison with the free drug at comparable concentration (1 μM) (Fig. 3).

After 48 h incubation, MCM41-NH_2/complex(**1**) reduced cell viability of 30%, and its cytotoxic effect increased with the time of treatment, causing about 50% of cell death in 72 h. When compared with free complex(**1**), antiproliferative efficacy of MCM41-NH_2/complex(**1**) appeared 30% lesser. On the contrary, MCM41/complex(**1**) caused only a slight, time-independent reduction of MCF-7 cell viability (15%), indicating that the trapping into the mesochannels and the partial release of the drug, largely limit its anti-tumoral efficacy. Both the unloaded mesoporous silica powders did not influence cell proliferation at any time.

Cytotoxic activity against MCF-7 cells of complex(**1**) is associated to apoptosis [9,29]. To evaluate whether the loading procedure into the silica carriers and subsequent release of the drug modified its biological activity, flow cytometry analysis for Annexin V binding and PI uptake of MCF-7 cells after treatment with complex(**1**) loaded into mesoporous silica nanoparticles, was carried out (Fig. 4). After 48 h incubation, whereas MCM41/complex(**1**) did not cause a significant change of the cellular state compared to control, MCM41-NH_2/complex(**1**) induced a clear shift of viable cells towards early apoptosis, similarly to the free drug.

4. Conclusions

The complex(**1**) encapsulation efficiency % (EE%) was 63.3 w/w% for the MCM41 and 94.4 w/w % for MCM41-NH_2 samples, respectively. After the loading, the surface area and the pore volume of MCM41 significantly decrease, indicating the presence of the drug within the pores. Instead different results were obtained for the MCM41-NH_2. A different mode of anchoring was guessed for MCM41-NH_2 that generates a coordination bond between the lone pair of –NH_2 group of mesoporous silica and Pt(II) ion of the complex(**1**) after dissociation of DMSO ligand. Therefore, the different release occurs for the different interactions between the drug and the functional groups of the mesoporous. While MCM41/complex(**1**) causes a slight, time-independent reduction of the MCF-7 cell viability, MCM41-NH_2/complex(**1**) markedly affects the tumour cell proliferation, longer the time treatment, stronger the inhibitory effect is. Then cytotoxicity of silica loaded complex(**1**) matches the release kinetic of the drug from the two different mesoporous matrices. Moreover, our results illustrate that pro-apoptotic efficacy of MCM41-NH_2/complex(**1**) is comparable to that of the free drug, indicating that mesoporous silica functionalized with amino groups is a good delivery matrix for the synthesized platinum complex. The percentage of release of complex(**1**) from the two systems are quite similar, thus the antitumor efficacy of MCM41/complex(**1**) may not be connected only to the partial release of the drug and to the trapping into the mesochannels. The results obtained will be the subject of future studies.

Acknowledgements

Financial support by the Ministero dell'Istruzione, dell'Università e della Ricerca, Italy, and by the Università di Palermo is gratefully acknowledged.

Appendix A. Supplementary data

Supplementary data associated with this article can be found, in the online version, at https://doi.org/10.1016/j.poly.2018.07.006.

References

[1] S. Rubino, V. Di Stefano, A. Attanzio, L. Tesoriere, M.A. Girasolo, F. Nicolò, G. Bruno, S. Orecchio, G.C. Stocco, Synthesis, spectroscopic characterization and antiproliferative Activity of two platinum(II) complexes containing N-donor heterocycles, Inorg. Chim. Acta 418 (2014) 112.
[2] S. Rubino, I. Pibiri, A. Attanzio, S. Orecchio, S. Buscemi, M.A. Girasolo, V. Di Stefano, L. Tesoriere, Synthesis of platinum complexes with 2-(5-perfluoroalkyl-1,2,4-oxadiazol-3yl)-pyridine and 2-(3-perfluoroalkyl-1-methyl-1,2,4-triazole-5yl)-pyridine ligands and their in vitro antitumor activity, J. Inorg. Biochem. 155 (2016) 92.
[3] J.M. Salas, M.A. Romero, M.P. Sánchez, M. Quirós, Metal complexes of [1, 2, 4]triazole-[1, 5-a]pyrimidine derivatives, Coord. Chem. Rev. 193–195 (1999) 1119.
[4] C. Marzano, D. Fregona, F. Baccichetti, A. Trevisan, L. Giovagnini, F. Bordin, Cytotoxicity and DNA damage induced by a new platinum(II) complex with pyridine and dithiocarbamate, Chem. Biol. Interact. 140 (2002) 215.
[5] G. Faraglia, D. Fregona, S. Sitran, L. Giovagnini, C. Marzano, F. Baccichetti, U. Casellato, R. Graziani, Platinum(II) and palladium(II) complexes with dithiocarbamates and amines: synthesis, characterization and cell assay, J. Inorg. Biochem. 83 (2001) 31.
[6] R.S. Keri, M.R. Patil, S.A. Patil, S.S. Budagumpi, A comprehensive review in current developments of benzothiazole-based molecules in medicinal chemistry, Eur. J. Med. Chem. 89 (2015) 207.
[7] A. Zablotskaya, I. Segal, A. Geronikaki, T. Eremkina, S. Belyakov, M. Petrova, I. Shestakova, L. Zvejniece, V. Nikolajeva, Synthesis, physicochemical characterization, cytotoxicity, antimicrobial, anti-inflammatory and

psychotropic activity of new *N*-[1,3-(benzo)thiazol-2-yl]-ω-[3,4-dihydroisoquinolin-2(1*H*)-yl]alkanamides, Eur. J. Med. Chem. 70 (2013) 846.
[8] M.K. Singh, R. Tilak, G. Nath, S.K. Awasthi, A. Agarwal, Design, synthesis and antimicrobial activity of novel benzothiazole analogs, Eur. J. Med. Chem. 63 (2013) 635.
[9] S. Rubino, R. Busà, A. Attanzio, R. Alduina, V. Di Stefano, M.A. Girasolo, S. Orecchio, L. Tesoriere, Synthesis, properties, antitumor and antibacterial activity of new Pt(II) and Pd(II) complexes with 2,2′-dithiobis(benzothiazole) ligand, Bioorg. Med. Chem. 25 (2017) 2378.
[10] M. Iafisco, N. Margiotta, Silica xerogels and hydroxyapatite nanocrystals for the local delivery of platinum-bisphosphonate complexes in the treatment of bone tumors: a mini-review, J. Inorg. Biochem. 117 (2012) 237.
[11] W.A. Wani, S. Prashar, S. Shreaz, S. Gómez-Ruiz, Nanostructured materials functionalized with metal complexes: In search of alternatives for administering anticancer metallodrugs, Coord. Chem. Rev. 312 (2016) 67.
[12] Z. Tao, B. Toms, J. Goodisman, T. Asefa, Mesoporous silica microparticles enhance the cytotoxicity of anticancer platinum drugs, ACS NaNo 4 (2010) 789.
[13] J. Gu, S. Su, Y. Li, Q. He, J. Zhong, J. Shi, Surface modification-complexation strategy for cisplatin loading in mesoporous nanoparticles, J. Phys. Chem. Lett. 1 (2010) 3446.
[14] C.H. Lin, S.H. Cheng, W.N. Liao, P.R. Wei, P.J. Sung, C.F. Weng, C.H. Lee, Mesoporous silica nanoparticles for the improved anticancer efficacy of cisplatin, Int. J. Pharm. 429 (2012) 138.
[15] M. Sguizzato, R. Cortesi, E. Gallerani, M. Drechsler, L. Marvelli, P. Mariani, F. Carducci, R. Gavioli, E. Esposito, P. Bergamini, Solid lipid nanoparticles for the delivery of 1,3,5-triaza-7-phosphaadamantane (PTA) platinum (II) carboxylates, Mater. Sci. Eng. C 74 (2017) 357.
[16] M. Vallet-Regí, A. Rámila, R.P. del Real, J. Pérez-Pariente, A new property of MCM-41: drug delivery system, Chem. Mater. 13 (2) (2001) 308.
[17] M. Ciabocco, P. Cancemi, M.L. Saladino, E. Caponetti, R. Alduina, M. Berrettoni, Synthesis and antibacterial activity of Iron Hexacyanocobaltate particles, J. Biol. Inorg. Chem. 23 (3) (2018) 385.
[18] M. Vallet-Regí, F. Balas, D. Arcos, Mesoporous materials for drug delivery, Angew. Chem., Int. Ed. 46 (2007) 7548.
[19] S.P. Hudson, R.F. Padera, R. Langer, D.S. Kohane, The biocompatibility of mesoporous silicates, Biomaterials 29 (2008) 4045.
[20] E. Caponetti, L. Pedone, M.L. Saladino, D. Chillura Martino, G. Nasillo, MCM-41-CdS nanoparticles composite material: preparation and characterization, Micropor, Mesopor. Mat. 128 (2010) 101.
[21] M.L. Saladino, A. Spinella, E. Caponetti, A. Minoja, Characterization of Nd-MCM41 obtained by impregnation, Micropor. Mesopor. Mater. 113 (2008) 490.
[22] E. Kraleva, M.L. Saladino, A. Spinella, G. Nasillo, E. Caponetti, $H_3PW_{12}O_{40}$ supported on mesoporous MCM-41 and Al-MCM-41 materials: preparation and characterization, J. Mater. Sci. 46 (22) (2011) 7114.
[23] S. Brunauer, P.H. Emmett, E. Teller, Adsorption of gases in multimolecular layers, J. Am. Chem., Soc. 60 (1938) 309.
[24] M.L. Saladino, S. Rubino, P. Colomba, M.A. Girasolo, D.F. Chillura Martino, C. Demirbag, E. Caponetti, Pt(II) complex @mesoporous silica: preparation, characterization and study of release, Biointerface Res. Appl. Chem. 6 (2016) 1621, and references therein.
[25] S.J. Gregg, K.S.W. Sing, Adsorption, Surface Area and Porosity, second ed., Academic Press, London, 1982.
[26] W. Zeng, X.F. Qian, Y.B. Zhang, J. Yin, Z.Z. Zhu, Organic modified mesoporous MCM41 through solvothermal process as drug delivery system, Mater. Res. Bul. 40 (2005) 766–772.
[27] K. Mori, K. Watanabe, M. Kawashima, M. Che, H. Yamashita, Anchoring of Pt(II) Pyridyl complex to mesoporous silica materials: enhanced photoluminescence emission at room temperature and photooxidation activity using molecular oxygen, J. Phys. Chem. C 115 (2011) 1044.
[28] J. Gu, J. Liu, Y. Li, W. Zhao, J. Shi, One-pot synthesis of mesoporous silica nanocarriers with tunable particle sizes and pendent carboxylic groups for cisplatin delivery, Langmuir 29 (2013) 403.
[29] A. Attanzio, M. Ippolito, M.A. Girasolo, F. Saiano, A. Rotondo, S. Rubino, L. Mondello, M.L. Capobianco, P. Sabatino, L. Tesoriere, G. Casella, Anti-cancer activity of di- and tri-organotin(IV) compounds with D-(+)-Galacturonic acid on human tumor cells, J. Inorg. Biochem. (2018), https://doi.org/10.1016/j.jinorgbio.2018.04.006.